Biomedicine & Pharmacotherapy 164 (2023) 114927

Contents lists available at ScienceDirect

Biomedicine & Pharmacotherapy

journal homepage: www.elsevier.com/locate/biopha

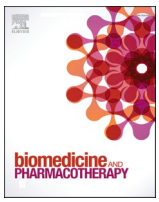

Gene expression profiling in white blood cells reveals new insights into the molecular mechanisms of thalidomide in children with inflammatory bowel disease

Letizia Pugnetti [a,1], Debora Curci [b,1], Carlotta Bidoli [c], Marco Gerdol [c], Fulvio Celsi [b], Sara Renzo [d], Monica Paci [d], Sara Lega [b], Martina Nonnis [b], Alessandra Maestro [b], Liza Vecchi Brumatti [b], Paolo Lionetti [d,e], Alberto Pallavicini [c], Danilo Licastro [f], Paolo Edomi [c], Giuliana Decorti [a,b], Gabriele Stocco [a,b], Marianna Lucafò [c,*], Matteo Bramuzzo [b]

[a] Department of Medicine, Surgery and Health Sciences, University of Trieste, Italy
[b] Institute for Maternal and Child Health, IRCCS "Burlo Garofolo", 34137 Trieste, Italy
[c] Department of Life Sciences, University of Trieste, 34127 Trieste, Italy
[d] Gastroenterology and Nutrition Unit, Meyer Children's Hospital IRCSS, 50139 Florence, Italy
[e] Department NEUROFARBA, University of Florence, 50139 Florence, Italy
[f] AREA Science Park, Padriciano 99, 34149 Trieste, Italy

ARTICLE INFO

Keywords:
Thalidomide
Pediatric
Crohn's disease
Ulcerative colitis

ABSTRACT

Thalidomide has emerged as an effective immunomodulator in the treatment of pediatric patients with inflammatory bowel disease (IBD) refractory to standard therapies. Cereblon (CRBN), a component of E3 protein ligase complex that mediates ubiquitination and proteasomal degradation of target proteins, has been identified as the primary target of thalidomide. CRBN plays a crucial role in thalidomide teratogenicity, however it is unclear whether it is also involved in the therapeutic effects in IBD patients. This study aimed at identifying the molecular mechanisms underpinning thalidomide action in pediatric IBD. In this study, ten IBD pediatric patients responsive to thalidomide were prospectively enrolled. RNA-sequencing (RNA-seq) analysis and functional enrichment analysis were carried out on peripheral blood mononuclear cells (PBMC) obtained before and after twelve weeks of treatment with thalidomide. RNA-seq analysis revealed 378 differentially expressed genes before and after treatment with thalidomide. The most deregulated pathways were cytosolic calcium ion concentration, cAMP-mediated signaling, eicosanoid signaling and inhibition of matrix metalloproteinases. Neuronal signaling mechanisms such as CREB signaling in neurons and axonal guidance signaling also emerged. Connectivity Map analysis revealed that thalidomide gene expression changes were similar to those exposed to MLN4924, an inhibitor of NEDD8 activating enzyme, suggesting that thalidomide exerts its immunomodulatory effects by acting on the ubiquitin-proteasome pathway. In vitro experiments on cell lines confirmed the effect of thalidomide on candidate altered pathways observed in patients. These results represent a unique resource for enhanced understanding of thalidomide mechanism in pediatric patients with IBD, providing novel potential targets associated with drug response.

1. Introduction

Inflammatory bowel disease (IBD), including Crohn's disease (CD) and ulcerative colitis (UC), are chronic inflammatory disorders of the intestinal tract, characterized by relapses and remissions, in which complex interactions among genetic, immune, and environmental factors are involved [1]. IBD is most often diagnosed in adolescence and early adulthood, with increasing incidence in the pediatric population [2,3]. Children with IBD tend to present with more extensive anatomic involvement, more severe disease course and often require more

* Corresponding author.
E-mail address: mlucafo@units.it (M. Lucafò).
[1] These authors have contributed equally to this work.

https://doi.org/10.1016/j.biopha.2023.114927
Received 14 March 2023; Received in revised form 9 May 2023; Accepted 22 May 2023
Available online 29 May 2023

aggressive treatment compared to patients with adult-onset disease [4]. A curative therapy does not presently exist, and medical treatment aims at inducing clinical remission by controlling inflammation and symptoms and maintaining remission to prevent relapses [5,6]. However, significant inter-individual variability is present, and many patients do not adequately respond to standard therapies and experience severe drug induced adverse events [7,8]. In the late 1950 s, thalidomide was prescribed to pregnant women as a sedative and as treatment against morning sickness, but was found to be teratogenic, causing severe birth defects [9]. Despite thalidomide's tragic history, the discovery of its immunomodulatory, anti-tumour necrosis factor (TNF-α) and anti-angiogenic properties renewed interest in this drug [10]. Thalidomide has been successful used for the treatment of erythema nodosum leprosum and multiple myeloma [11], and it has been shown to be an effective treatment for IBD patients refractory to standard therapies, particularly in the pediatric population [12–15]. Thalidomide long-term use is often limited by its safety profile: peripheral neuropathy is the main adverse drug reaction and is a common cause of treatment discontinuation [16]. However, molecular information on thalidomide-induced peripheral neuropathy mostly derives from studies on patients with multiple myeloma [17], and few data have been reported about the causes that trigger this adverse reaction in pediatric patients with IBD. In 2010, cereblon (CRBN), a substrate receptor component of E3 protein ligase complex that mediates the ubiquitination and proteasomal degradation of target proteins, was identified as the primary target of this drug [18]. CRBN interacts with DNA damage binding protein 1 (DDB1) to form the ubiquitin E3 ligase complex cullin-4A (CUL4A)/RING-box protein 1 (RBX1) - DDB1-CRBN (CRL4A-CRBN). As a substrate receptor, CRBN recruits target substrates to cullin-RING ubiquitin E3 ligase 4 A (CRL4A), mediating the ubiquitination and proteasomal degradation of target proteins [19]. Thalidomide and its derivatives bind CRBN and inhibit or promote ubiquitination of target substrates such as the Cys2-His2 (C2H2) zinc finger proteins Ikaros and Aiolos by CRL4A-CRBN in multiple myeloma [20–24], however it is not clear if this mechanism is involved also in the therapeutic effects in IBD patients. Furthermore, thalidomide inhibits selectively TNF-α expression by enhancing mRNA degradation [25] and suppresses NF-κB activation, preventing its DNA binding activity [26]. However, the molecular mechanism of action of thalidomide in IBD pediatric patients is not fully understood and transcriptomic studies in pediatric patients are still missing.

The aim of this research is to fill in the knowledge gaps of the therapeutic mechanism of action of thalidomide in IBD pediatric patients, providing new insight for the identification of molecular markers useful for the identification of new immunosuppressive mechanism in pediatric IBD and prospectively for the personalization of therapy.

2. Materials and methods

2.1. Patient population

Ten IBD pediatric patients (mean age at enrolment 13.1 years, 6 CD, 6 males) refractory to previous pharmacological therapies were prospectively enrolled at the Institute for Maternal and Child Health IRCCS "Burlo Garofolo" in Trieste and the "Meyer" Children's Hospital in Florence, Italy. Patients were treated with thalidomide at the dose of 1.5–2.5 mg/kg/day for 12 weeks. Clinical activity was assessed using the "Pediatric Crohn's Disease Activity Index" (PCDAI) for patients with Crohn's disease, and the "Pediatric Ulcerative Colitis Activity Index" (PUCAI) for patients with ulcerative colitis. All patients showed an improvement of symptoms after treatment at week 12 with PCDAI or PUCAI < 10. Peripheral blood was obtained before (pre-treatment, PRE) and after 12 weeks of treatment (post-treatment, POST) for RNA extraction and transcriptomic analysis.

2.2. RNA extraction

Peripheral blood mononuclear cells (PBMCs) were collected by density gradient centrifugation on Ficoll PaqueTM Plus (Healthcare, Milan, Italy) before (PRE) and after 12 weeks (POST) of therapy. The PBMCs were preserved in TRIzol (Thermo Scientific, Waltham, MA, USA) at – 80 °C up to the RNA extraction, which was done with the PureLink RNA Mini kit (Thermo Scientific, Waltham, MA, USA), according to the manufacturer's protocol. The total RNA concentration and purity were determined by NanoDrop instrument (NanoDrop 2000, Thermo Scientific, Waltham, MA, USA). The absence of significant degradation of extracted RNAs was evaluated through the calculation of RNA Integrity Number with an Agilent BioAnalyzer (Agilent, Santa Clara, CS, USA) instrument. All samples met the quality requirements to allow the preparation of Illumina sequencing libraries.

2.3. RNA-sequencing

The RNA samples were shipped to the Institute for Applied Genomics (IGA, Udine, Italy), which carried out library preparation using the Illumina TruSeq kit following the manufacturer's instructions with a poly-A enrichment strategy. The libraries were subjected to paired-end (PE) sequencing on an Illumina Hiseq 2000 platform with a 2×150 paired-end strategy. Raw sequencing data were processed with the CLC Genomics WorkBench v.20 (Qiagen, Hilden, Germany), to remove low quality reads, ambiguous nucleotides, residual adapters and reads shorter than 30 nucleotides. Trimmed reads obtained from each sample were independently mapped on the annotated human genome (Ensembl release 68) using the *RNA-Seq Analysis* tool included in CLC Genomics WorkBench, with *length fraction* and *similarity fraction* parameters set to 0.98. The gene expression levels have been reported as Transcripts Per Million (TPM) to ensure full comparability among samples [27]. The RNA-seq study has been deposited at the NCBI BioProject archive under the accession ID PRJNA818525.

2.4. Differential gene expression analysis

The expression values calculated for each sample were used as an input for the statistical analysis of differential gene expression (DGE), carried out with the CLC Genomics Workbench v.20, which implements a generalized linear model. In detail, PRE and POST samples were considered as two different groups in a pairwise comparison. This analysis tested the effects of the treatment on gene expression, while controlling for inter-individual variation, regardless of the CD or UC diagnosis. The differentially expressed genes (DEGs) were selected based on a False Discovery Rate (FDR)-corrected p-value threshold < 0.05, combined with a fold change (FC) threshold > 2 (for up-regulated DEGs) and < -2 (for down-regulated DEGs).

The list of DEGs was subjected to a hierarchical clustering analysis, based on Euclidean distance and complete linkage, which clustered both the DEGs and the samples based on gene expression trend similarities.

Two additional DGE analyses were carried out considering separately the subgroups of CD and UC patients, using the same methodology and significance thresholds detailed above for the full dataset including all IBD patients.

2.5. Functional enrichment analysis

The differential analyses were integrated with functional enrichment analyses, implemented in a hypergeometric test [28], carried out on the Gene Ontology (GO) annotations associated with each DEG. The GO terms which displayed an FDR-adjusted p-value < 0.05 and a difference between the number of *observed and expected* occurrences for each term > 3 were considered as significantly enriched in each subset of DEGs.

The list of DEGs identified in the complete set of all IBD patients was further analyzed with the QIAGEN Ingenuity Pathway Analysis [29]

software (Qiagen, Hilden, Germany) with the aim to investigate enriched pathways in association with differential expression and predict their activation or repression state, based on their z-score value. For each canonical pathway, the Fisher's exact test p-value was calculated to measure the statistical significance of enrichment in DEGs of the pathway. Moreover, the ratio of the number of DEGs that are in the pathway to the total number of gene involved in the pathway was calculated. Both the p-value and the ratio indicate the impact of the altered molecular expression on the functional pathways.

In addition, the DEGs list was also used to predict the possible involvement of upstream regulators and to provide an estimate of the downstream biological effects listed in the Diseases and Bio Function categories. The most significant canonical pathways identified by Ingenuity Pathway Analysis (IPA) were graphically displayed as networks, representing the interactions between molecules and the downstream biological functions; a few selected upstream regulators of particular interest due to their relevance in the biological context of this experiment were included.

2.6. Connectivity Map analysis

The top 150 most significant up-regulated and top 150 most significant down-regulated genes were selected for the implementation of the Connectivity Map (CMap) analysis [30]. The CMap database collects gene-expression profiles induced by exposing different cell types to various compounds, thus representing a popular resource for drug repositioning. In this case, it allowed to identify similarities between the alterations of the gene-expression profiles induced by thalidomide and those induced by the exposure to other perturbagens. The resulted perturbagens were filtered based on an arbitrary score threshold > 50, indicating correlation with the alterations induced by thalidomide.

2.7. Cell cultures and differentiation

THP-1 monocytic cell line (ATCC, TIB-202) was grown in RPMI 1640 medium (EuroClone®, Milan, Italy). SHSY-5Y neuroblastoma cell line (catalogue number 94030304, Sigma-Aldrich, Saint Louis, MO, USA) was maintained in Dulbecco's Modified Eagle's Medium/Nutrient Mixture F-12 Ham (Sigma-Aldrich, Saint Louis, MO, USA), supplemented with non-essential amino acid (10 mM for each amino acid; Sigma-Aldrich, Saint Louis, MO, USA). All media were supplemented with 10% (v/v) fetal bovine serum (FBS, Sigma-Aldrich, Saint Louis, MO, USA), 1% (v/v) L-glutamine 20 nM, 1% (v/v) penicillin 10,000 UI/mL and streptomycin 10 mg/mL (EuroClone®, Pero, Milan, Italy). Cell cultures were maintained according to standard procedures in a humidified incubator at 37 °C with 5% CO_2, and cells were passaged twice a week.

THP-1 cells were differentiated into macrophages using 5 ng/mL of phorbol-12-myristate 13-acetate (PMA, Sigma-Aldrich, Saint Louis, MO, USA) for 48 h. Monocytes and macrophages were stimulated with lipopolysaccharide (LPS; Thermo Fisher Scientific, Waltham, MA, USA) 1 μg/mL for 3 h [31].

To induce differentiation of SHSY-5Y cell line into a neuron-like phenotype cell with neurite outgrowth and branches, one day after plating cells were incubated in Neurobasal medium (Gibco, Thermo Fisher Scientific, Waltham, MA, USA), supplemented with B-27 supplement (Gibco, Thermo Fisher Scientific, Waltham, MA, USA) and L-glutamine (EuroClone®, Milan, Italy). Dibutyryl cyclic AMP 1 mM (DbcAMP; Sigma-Aldrich, Saint Louis, MO, USA) was added to the medium for 3 days [32].

2.8. Cytotoxicity assay

MTT (3,4-dimethylthiazole-2,5-diphenyltetrazolium bromide) (Sigma-Aldrich, Saint Louis, MO, USA) assay test was used to quantify the possible cytotoxic effect of thalidomide. Cells were treated with different concentrations (50, 100, 200, 400 μM) of thalidomide for 72 h. Four hours before treatment expiry, cells were incubated with MTT and finally levels of MTT/formazan were determined by measuring the absorbance at the double wavelength of 540 and 630 nm.

2.9. Real-time PCR

Expression levels of the most significant downregulated genes (*ADAMTS2* and *CELSR2*) were evaluated by real-time RT-PCR SYBR Green and TaqMan® analysis respectively, using the CFX96 real-time system-C1000 Thermal Cycler (Bio-Rad Laboratories, Hercules, CA, USA). The reverse transcription reaction was carried out with the High Capacity RNA-to-cDNA Kit (Applied Biosystems™, Carlsbad, CA, USA) and the real-time PCR was performed in triplicate using the Predesigned KiCqStart® SYBR® Green Primers (FH1_ADAMTS2 and FH1_ACTB; Sigma-Aldrich, Saint Louis, MO, USA) and TaqMan® Gene Expression Assay (Applied Biosystems, Carlsbad, CA, USA, Cat. N. 4331182, actin beta, ACTB ID: Hs01060665_g1; CELSR2 ID: Hs00154903_m1) according to the manufacturer's instructions.

The expression levels were determined using the Ct method ($2^{-\Delta\Delta CT}$). Gene expression values were normalized using *ACTB* as reference gene.

2.10. Enzyme-linked immunosorbent assays (ELISA)

ELISA assay was performed for the quantification of PGE2 and cAMP on supernatants of THP-1 cells. For PGE2 quantification, Prostaglandin E2 Elisa kit-monoclonal (Cayman Chemical, Michigan, USA) was used. For cAMP quantification, cAMP Elisa kit (Cayman Chemical, Michigan, USA) was used. The absorbance was measured by the GloMax-Multi Detection System (Promega, Milan, Italy).

2.11. Adenosine triphosphate (ATP) determination

SHSY-5Y cells were seeded in 96 well plates and, after 24 h of colture, were stimulated for 72 h with thalidomide (50–200 μM). After incubation, cells were lysed using 100 μl of PBS with 0.02% of TritonX100. ATP was measured using the ATP determination kit (Invitrogen, ThermoFisher, Waltham, MA, USA) following manufacturer instruction in 10 μl of the lysates and the luminescence was read with the GloMax-Multi Detection System (Promega, Milan, Italy) and expressed as ATP concentration using the standard provided by the kit. ATP level was normalized on protein concentration.

2.12. Mitochondrial membrane potential and reactive oxygen species measurement

To measure mitochondrial membrane potential (MMP) and reactive oxygen species (ROS) production, SHSY-5Y cells were seeded in 96 well plates and, after 24 h, cells were treated for 72 h with thalidomide (50–400 μM). After drug exposure, MMP and ROS were measured. For MMP, JC-1 probe (Sigma-Aldrich, Saint Louis, MO, USA) was used, loading cells with probe (10 μM) for 30 min at 37 °C, and then the fluorescence was read immediately. The results were expressed as green (525 nm) to red (590 nm) fluorescence intensity ratio normalized on untreated cells. For ROS quantification, CellROX Green Reagent (Invitrogen, ThermoFisher, Waltham, MA, USA), a cell-permeant dye, was added to each well at a concentration of 10 μmol/L. After 30 min of incubation, fluorescence was measured at the GloMax-Multi Detection System (Promega, Milan, Italy). The dye is weakly fluorescent when in a reduced state and exhibits green fluorescence upon oxidation, with absorption/emission maxima of 485/520 nm. ROS levels were normalized on protein concentration.

2.13. Intracellular calcium quantification

To evaluate the effect of thalidomide on intracellular calcium levels, Fluo-4 acetoxymethyl ester (Fluo-4 AM), a cell-permeant dye (ThermoFisher, Waltham, MA, USA) was used to test the effect of this drug on intracellular calcium. SHSY-5Y, treated with thalidomide at different concentrations (50–200 μM) for 72 h, were loaded with the dye (10 μM) for 30 min at 37 °C and then the fluorescence was analyzed with Cytation5 (Agilent BioTek, Santa Clara, CA, USA). Fluorescence was read by excitation at 485 nm, and emission at 520 nm, measuring every 0.2 s. After 60 s, an automated dispenser was used to distribute 10 μL of thapsigargin, a non-competitive inhibitor of the sarco/endoplasmic reticulum Ca^{2+} ATPase (SERCA), (10 Mm; Sigma Aldrich, Saint Louis, MO, USA) in each well and followed by continuous fluorescence monitoring. Fluorescence reads, normalized on baseline (means of first 20 s readings) were reported as maximum normalized fluorescence after thapsigargin stimulation. Untreated cells were used as control.

2.14. Immunoblot assay

Total cell extracts were prepared in RIPA buffer without SDS (150 mM NaCl, 50 mM Tris-HCl Ph8, 1 mM EDTA, 1% NP-40, 0.5% Na-deoxycholate) supplemented with protease inhibitor cocktail 1X (ThermoFisher, Waltham, MA, USA). After sonication, protein concentrations were determined by BCA assay using bovine serum albumin as standard. Twenty micrograms of lysates were loaded on Sodium Dodecyl Sulphate – Polyacrylamide Gel Electrophoresis (SDS-PAGE) 4–12% gradient gels (NUPAGE 4–12%, Bis-Tris Plus Gels, ThermoFisher, Waltham, MA, USA) and transferred, in wet condition, onto a nitrocellulose membrane.

Afterwards, each sample was incubated with 5% milk solution in T-TBS (10 mM Tris-HCl Ph 8, 150 mM NaCl; 0.1% Tween 20) for 1 h at 4 °C on a rocking platform. After blocking, incubation with the following primary antibodies, diluted 1:1000, was performed overnight, at 4 °C: anti-GAPDH rabbit (Cell Signaling Technologies, Danvers, MA, USA); anti-CREB rabbit (Cell Signaling Technologies, Danvers, MA, USA) and anti-phospho-CREB rabbit (Cell Signaling Technologies, Danvers, MA, USA).

Anti-rabbit HRP conjugated (OriGene technologies, Rockville, MD, USA) secondary antibodies were incubated for 1 h at 4 °C. Proteins were detected by chemiluminescence using a ChemiDoc system (Bio-Rad Laboratories, Hercules, CA, USA) and the band's density was analyzed using the ImageJ program. All data were normalized on GAPDH.

2.15. Statistical analysis

Statistical analyses were performed using GraphPad Prism. One and Two-way ANOVA with Tukey's multiple comparison test were used for the analysis of gene and protein expression, for ELISA assays, for measurement of intracellular ATP, calcium quantification analysis, quantification of ROS, MMP and for MTT assay. P-value < 0.05 was considered statistically significant.

3. Results

3.1. RNA-sequencing

To investigate thalidomide mechanism in responsive pediatric IBD patients (including both CD and UC diagnoses), we first performed a transcriptome analysis generated from a total of 20 paired PBMCs samples obtained before and after treatment. Differential expression analysis was performed on paired samples collected pre-treatment (PRE) and post-treatment (POST). The statistical analysis of differential gene expression, based on nearly 400 million high quality Illumina reads (Data note S1), highlighted a number of genes that underwent significant expression shifts in response to treatment. A total of 378 differentially expressed genes (DEGs) were identified (absolute fold change > 2, FDR adjusted p-value < 0.05), consisting of 229 up-regulated genes and 149 down-regulated genes. (Fig. 1, Table S1). An in-depth view of the DEGs specifically modulated in CD and UC patients is provided in Data note S1.

3.2. Gene ontology (GO) and Ingenuity Pathway Analysis (IPA)

The association between the differentially expressed genes detected in the complete dataset of IBD patients and significantly enriched annotations based on GO database was investigated with a hypergeometric test. This analysis allowed the identification of 151 significantly enriched terms, of which 89 represent biological processes (BP), 32 represent molecular functions (MF) and 30 represent cellular components (CC) (Fig. 2A, Table S2). Among MF, the most enriched terms regarded in particular "transmembrane signaling receptor activity" and "chemokine receptor activity". Consistently with these observations, the GO terms "chemokine-mediated signaling pathway" and "chemotaxis" were listed among the top enriched BP (Fig. 2A). Other important enriched BPs in the context of IBD and thalidomide immunomodulator activity were "inflammatory response", "immune response", "cell-cell adhesion" and "extracellular matrix organization". The analysis of CC revealed a highly significant enrichment of genes involved in integral component of "plasma membrane" and "collagen-containing extracellular matrix", which are coherent with the enriched MF and BP described above (Fig. 2A).

Although the separate analyses of CD and UC patients revealed a relatively small overlap between the DEGs shared by the IBD subtypes (Fig. S1), the hypergeometric test on GO annotations highlighted a similar enrichment. Indeed, while CD and UC only shared a limited fraction of enriched GO categories (BP: 12.8%, CC: 26.2%, MF: 26.9%) the same high-tier GO macro-categories were represented in both subtypes (Fig. S2, Fig. S3).

An approach exploiting the IPA database allowed a better comprehension of the most significant biological interactions among the differentially expressed genes identified in all IBD patients. Consistently with the aforementioned GO enrichment test, several altered canonical pathways were associated with immune cells activity ("phagosome formation", "granulocyte adhesion and diapedesis", "crosstalk between dendritic cells and natural killer cells") (Table 1). Interestingly neuronal signaling mechanisms such as "CREB signalling in neurons", "axonal guidance signaling" and "GABA receptor signaling" (Fig. 2B, Table 1) also emerged. Among the most significantly enriched canonical pathways, "G-protein Coupled Receptor Signaling" (Fig. S4), "CREB Signaling in Neurons" (Fig. S5) and "Axonal Guidance Signaling (Fig. S6) were considered for graphical representation to highlight interactions between DEGs and the other molecules involved in the pathways.

IPA also allowed the identification of several upstream regulators, which can be considered as strong candidates responsible for the regulation of DEGs (Table 2). Several pro-inflammatory cytokines and pro-angiogenic factors known to be regulated by thalidomide, such as IL2, TNF, VEGF, and TGFB1, were identified as upstream regulators of DEGs in IBD patients.

The complete lists of Canonical Pathways and Upstream Regulators detected by IPA are available in Table S3 and Table S4 respectively.

3.3. Comparison of the transcriptional effects of thalidomide and other compounds

The CMap analysis allowed the identification of several compounds whose treatment was linked with gene expression signatures correlated with the one induced by thalidomide, among which 16 perturbagens resulted significant (Table 3). The genes commonly altered by thalidomide and the 16 compounds are reported in Table S5.

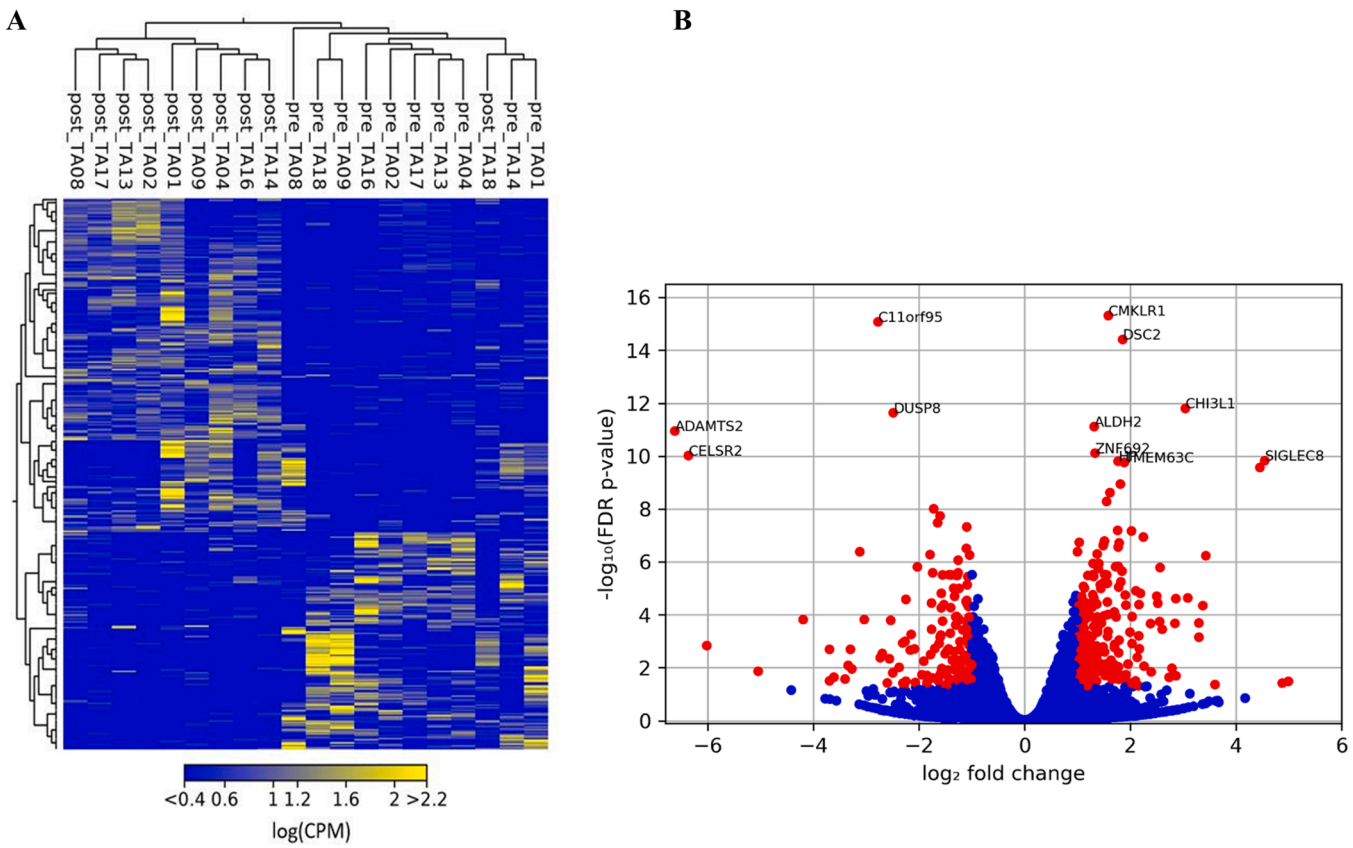

Fig. 1. A) Hierarchical clustering based on Euclidean distance and complete linkage of normalized log CPM (Counts Per Million) normalized expression values. Both the genes and the samples were subjected to hierarchical clustering based on the similarity of expression patterns. B) Volcano plot. The red dots represent significantly differentially expressed genes (absolute fold change > 2, FDR adjusted p-value < 0.05), and the blue dots represent non-significant differentially expressed genes.

3.4. Evaluation of the effect of thalidomide on the eicosanoid signaling: PGE2 quantification in THP1 cell line

After excluding potential cytotoxic effects of thalidomide on THP-1 and THP-1-derived macrophages by MTT test (Fig. S7), we investigated a possible involvement of pathways emerging from RNA-seq analysis in the mechanism of action of thalidomide starting from the prostaglandin's pathway. In particular, PGE2 production was quantified in THP-1 differentiated after treatment with thalidomide and LPS. As shown in Fig. 3, thalidomide reduced the production of PGE2 after co-stimulation with LPS in macrophages.

3.5. Evaluation of the effect of thalidomide on cAMP-mediating signaling in THP-1 cells

To study the possible alteration by thalidomide in cAMP related signaling pathways, the production of cAMP was quantified in THP-1 cells and in cells differentiated in macrophages, both treated with thalidomide and LPS.

The results indicate that, in monocytes, thalidomide induces a significant increase in cAMP production, in particular in cells co-treated with LPS and 200 μM of thalidomide (Fig. 4). Data obtained in macrophages are not shown because very low levels of cAMP were detected, out of the detection range of the ELISA kit used.

3.6. Cytotoxicity of thalidomide in SHSY-5Y cells: evaluation of metabolic activity and ROS production

The cytotoxicity of thalidomide in vitro was evaluated both in undifferentiated and differentiated SHSY-5Y cell lines. The data reported in Fig. 5 show that thalidomide does not cause changes in viability in the cell models tested at all concentrations.

The absence of cytotoxicity at the concentrations used was also confirmed by the analysis of mitochondrial membrane potential and ROS quantification in SHSY-5Y cells after treatment with the drug (Fig. 6). Interestingly, thalidomide induced a significant, although moderate increase in ATP production after the 72 h treatment (Fig. 7).

3.7. Validation of the top 2 downregulated genes by thalidomide in SHSY-5Y cellular model

The differential expression of the top 2 downregulated genes *ADAMTS2* and *CELSR2* measured by RNA-seq on PBMCs of IBD patients treated with thalidomide was further demonstrated in human neuroblastoma SHSY-5Y cell line treated with the drug (Fig. 8). In particular, *ADAMTS2* was downregulated in both undifferentiated and differentiated cell lines while *CELSR2* was significantly downregulated in the differentiated cell line (Fig. 8).

3.8. Intracellular calcium quantification in SHSY-5Y cell line

To monitor the changes in intracellular calcium, in particular the effect of the drug on calcium release from ER, the site of intracellular calcium storage, Fluo-4 AM was used as a fluorescent probe. To quantify the release of calcium from ER, thapsigargin, a non-competitive inhibitor of the sarco/endoplasmic reticulum Ca^{2+} ATPase (SERCA), was added.

As reported in Fig. 9, a significant change in intracellular calcium levels upon thapsigargin stimulation was evident, with a marked increase of Ca^{2+} peaks at all thalidomide concentrations used, suggesting

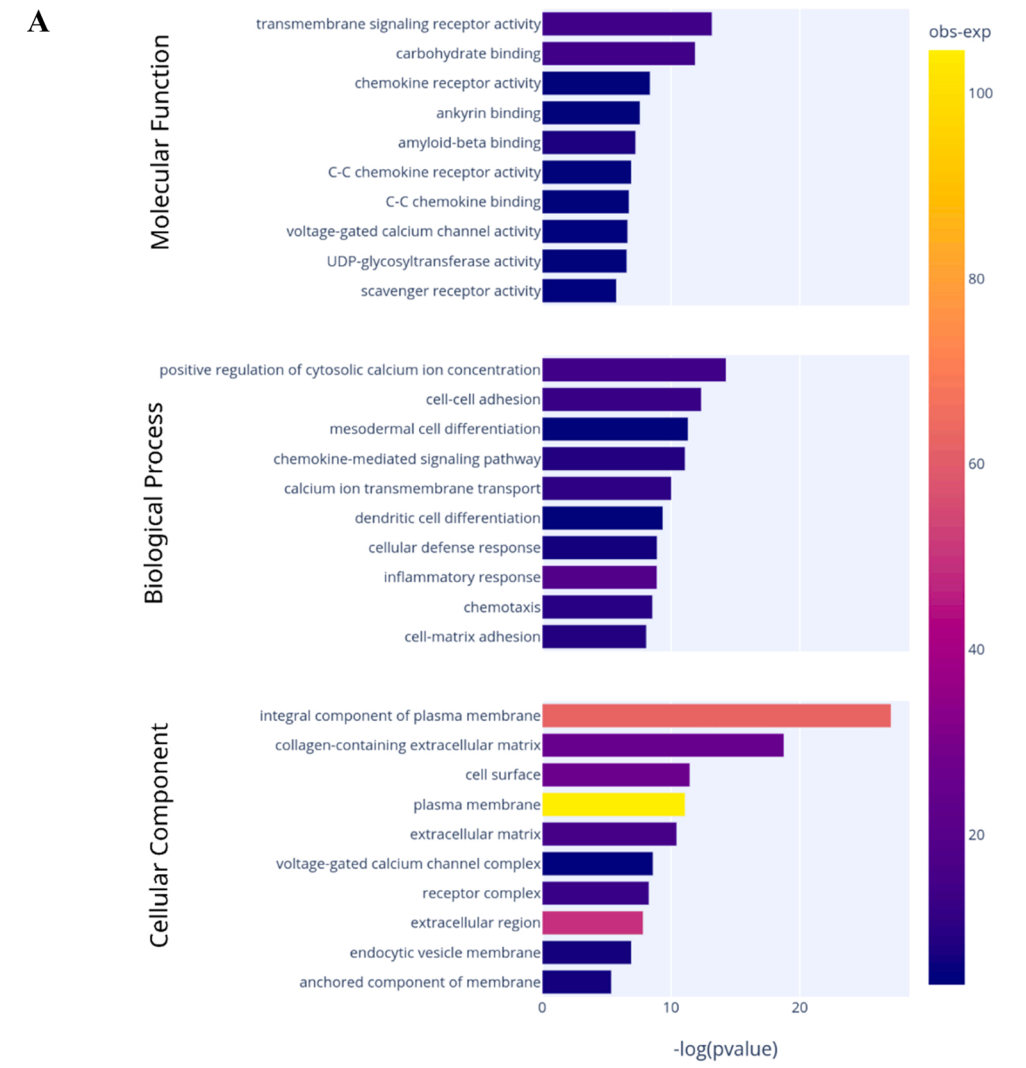

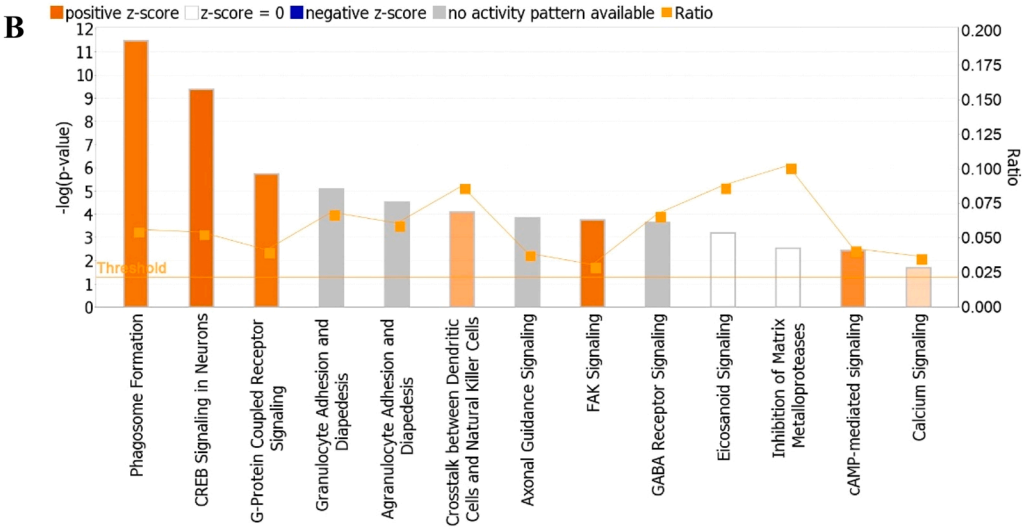

Fig. 2. A) The top 10 enriched terms in each category were displayed. Each histogram is referred to a Gene Ontology category (Biological process, Molecular function, Cellular component). GO terms are ranked according to the FDR adjusted p-value. B) Canonical pathways significantly enriched following ingenuity pathway analysis (IPA). The z-score indicates predicted activation state of the canonical pathway. Negative z-score corresponds to down-regulation of the pathway, while positive z-score corresponds to up-regulation of the pathway. Ratio denotes the number of significantly expressed genes compared with the total number of genes associated with the canonical pathway.

Table 1
IPA Enriched Canonical Pathways altered by thalidomide in pediatric patients with IBD. -log(p-value) describes the significance of the association of canonical pathways with differential expression. The greater the -log(p-value), the more significant the canonical pathway. The z-score is a statistical measure determined to assess prediction of activation (z-score > 0) or inhibition (z-score < 0) of biological functions; the pathways with no z-score could not be associated neither with activation nor with repression. Ratio indicates the number of observed genes that map to the pathway divided by the total number of expected genes that map to the same pathway.

Ingenuity Canonical Pathways	-log (p-value)	z-score	Ratio	DEGs
Phagosome Formation	11.4	2.40	0.06	*ADGRE1,ADORA3, ADRB2,CCR3,CCR8, CD209,CD36,CELSR1, CELSR2,CMKLR1, CX3CR1,CYSLTR2, FCER1A,FCGR3A/ FCGR3B,FFAR1,FFAR2, FN1,FZD4,GLP1R,GPR63, GPRC5A,HRH4,HTR1F, ITGA3,ITGA8,ITGAD, MARCO,MRAS,MSR1, MYL9,PLA2G7,PLAAT5, PLD5,PTGDR,PTGDR2, PTGER3,PTGFR,RXFP2, TLR3*
CREB Signaling in Neurons	9.37	2.61	0.05	*ADGRE1,ADORA3, ADRB2,CACNA1D, CACNA1I,CACNB4, CACNG6,CACNG8, CAMK2A,CCR3,CCR8, CELSR1,CELSR2, CMKLR1,CX3CR1, CYSLTR2,FFAR1,FFAR2, FGFR2,FLT4,FZD4, GLP1R,GPR63,GPRC5A, HRH4,HTR1F,MRAS, NTRK1,PTGDR,PTGDR2, PTGER3,PTGFR,RXFP2*
Granulocyte Adhesion and Diapedesis	5.07		0.07	*CCL4,CCR3,CCR8,CXCL1, CXCL9,CXCR5,HRH4, IL1RL1,MMP14,MMP28, MMP9,SDC2,XCL2*
Agranulocyte Adhesion and Diapedesis	4.5		0.06	*CCL4,CCR3,CCR8,CXCL1, CXCL9,CXCR5,FN1, ITGA3,MMP14,MMP28, MMP9,MYL9,XCL2*
Axonal Guidance Signaling	4.31		0.04	*ADAMTS1,ADAMTS17, ADAMTS2,FZD4,ITGA3, ITGA8,ITGAD,L1CAM, MME,MMP14,MMP28, MMP9,MRAS,MYL9, NTRK1,SDC2,SEMA3F, SLIT3,SRGAP1,WNT10A, WNT5B*
Crosstalk between Dendritic Cells and Natural Killer Cells	4.07	1.63	0.08	*CAMK2A,CD209,IL4, KIR2DL4,KIR3DL1, KLRD1,TLR3,TREM2*
GABA Receptor Signaling	3.63		0.07	*CACNA1D,CACNA1I, CACNB4,CACNG6, CACNG8,GABRE,KCNH2, MRAS,UBD*
Eicosanoid Signaling	3.19		0.09	*CYSLTR2,PLA2G7, PLAAT5,PTGDR,PTGER3, PTGFR*
Inhibition of Matrix Metalloproteases	2.52		0.1	*MMP14,MMP28,MMP9, SDC2*
Calcium Signaling	1.71	0.82	0.04	*CACNA1D,CACNA1I, CACNB4,CACNG6, CACNG8,CAMK2A,MYL9, TPM2*
FAK Signaling	0.96		0.03	*ITGA3,ITGA8,ITGAD, MRAS*

Table 2
Top 15 Upstream regulators determined by IPA. Activation z-scores infers the activation state of predicted regulators, where positive values correspond to an activated state and negative values to an inhibited state; p-value of overlap define the significance of overlapping between the set of genes and the genes targeted by the upstream regulator.

Upstream Regulator	Activation z-score	p-value of overlap	Target molecules (up DEGs)	Target molecules (down DEGs)
IL2	2.27	1.80E-10	*ANXA1, CCL4, CCR3, CCR8, CMKLR1, CX3CR1, DAPK2, EOMES, FGFR2, GATA1, GZMA, GZMB, HOPX, HRH4, IDO1, IL1RL1, IL4, KIR2DL4, KIR3DL1, KLRC1, KLRD1, KLRF1, LGALS12, MME, MMP9, PROK2, TNFRSF10C, TNFRSF9, XCL2*	*CXCR5, FCGR3A/ FCGR3B, HSPA1A/HSPA1B, L1CAM, LRRC32, RGPD4* (includes others), *TNFRSF13B, TNFRSF13C*
TNF	2.446	3.85E-10	*ADRB2, AKAP12, ALDH2, ANXA1, CABP1, CCL4, CCR3, CCR8, CD163, CD209, CD36, CHI3L1, CLEC5A, CMKLR1, CPA3, CX3CR1, CXCL1, CXCL9, CYYR1, DSC2, EGR1, FGFR2, GATA2, HDC, HOXA9, HP, IDO1, IGFBP2, IL1RL1, IL4, KL, LGALS12, MMP14, MMP9, NCAM1, PNPLA1, PROK2, PRSS23, PTGFR, RETN, RGS9, S100A12, SLC1A3, STAC, STEAP4, TLR3, TNFRSF9, TREM2, UBD, ZNF365*	*ARHGEF17, C15orf48, CAVIN3, CCN3, COL4A3, CXCR5, FFAR1, FLT4, FN1, HID1, HSPA1A/ HSPA1B, INHBA, KCNH2, MMP28, MSR1, PLEKHG1, PRTN3, SDC2, SYNGR3, WNT10A*
Vegf	1.751	3.44E-09	*ADAMTS1, AKAP12, ANGPT4, CHI3L1, CPA3, CXCL1, CYYR1, EGR1, GATA1, HDC, HOPX, IL4, IL5RA, KIR2DL4, MMP14, MMP9, NRG1, RGS9, TLR3, TNFRSF10C, TNFRSF9*	*ACAN, ARHGEF17, CELSR1, COL4A3, FLT4, FN1, HID1, INHBA, NRCAM*
GATA2	1.597	3.08E-08	*CCR3, CCR8, CD36, CES1, CHI3L1, CPA3, FCER1A, GATA1, GATA2, GZMA, HDC, HOXA10, IL1RL1, IL4, MCEMP1, MS4A2, NME8, RAB44, TSHB, UBXN10, ZNF365*	*CCN3, MATN1, PRTN3, SLC35D3*
IL4	1.479	5.05E-08	*ADGRE1, ALDH2, ANXA1, CCL4, CCR3, CCR8, CD163, CD209, CD36, CLEC10A, CXCL1, CXCL9, CYSLTR2, EOMES,*	*C15orf48, COBLL1, CXCR5, DNASE1L3, FCGR3A/FCGR3B, FN1, HSPA1A/ HSPA1B, KCNH2,*

(*continued on next page*)

Table 2 (*continued*)

Upstream Regulator	Activation z-score	p-value of overlap	Target molecules (up DEGs)	Target molecules (down DEGs)
			GZMA, HDC, HOPX, HP, IDO1, IL1RL1, IL4, IL5RA, KLRD1, MARCO, MMP9, MS4A2, PTGDR2, SOX13, TFEC, TMTC1, TNFRSF9, TPBG, TREM2, XCL2	*LRRC32, MMP28, MSR1, SYNGR3*
CSF2	2.64	8.43E-08	*ANXA1, CCL4, CD163, CD209, CX3CR1, CXCL1, EGR1, FFAR2, GATA1, HDC, HOXB4, HRH4, IDO1, IL1RL1, IL4, IL5RA, MARCO, MME, MMP14, MMP9, NCAM1, PNPLA1, PROK2, STEAP3, TNFRSF9, UBD*	*INHBA, MNS1*
TBX21	0.462	1.82E-07	*CCL4, CX3CR1, EOMES, GZMA, GZMB, IL1RL1, IL4, KLRD1, PTGDR2*	*CXCR5*
TGFB1	-1.305	1.91E-07	*ACVRL1, ALDH2, CCL4, CCR3, CD163, CD36, CDHR1, CHI3L1, CX3CR1, CXCL1, DSC2, EGR1, EOMES, FCER1A, FGFR2, GATA1, GZMA, GZMB, HOPX, IDO1, IGFBP2, IL1RL1, IL4, KL, KLRC1, KLRD1, MMP14, MMP9, MS4A2, NCAM1, NMNAT2, RETN, SERPINH1, SLIT3, TPM2, WNT5B, XCL2, ZNF365*	*ACAN, ADAMTS2, ANXA8/ ANXA8L1, CCN3, CELSR2, CRIP2, CXCR5, FBLN2, FCGR3A/FCGR3B, FGF9, FN1, GPRC5A, HAPLN3, HSPA1A/HSPA1B, HTRA1, INHBA, ITGA3, L1CAM, MSR1, PMEPA1, RNF152, SDC2, SPAG4, WNT10A*
IL6	3.547	4.79E-07	*ACVRL1, ADAMTS1, ADGRE1, ANXA1, CCL4, CCNA1, CCR3, CD163, CD209, CD36, CES1, CLEC10A, CX3CR1, CXCL1, EGR1, EOMES, FFAR2, GATA1, GZMB, HP, IDO1, IL1RL1, IL4, KLRD1, MMP9, PROK2, PTGFR, STEAP4, TLR3*	*FN1, LARGE1, MRAS, MSR1, PRTN3*
CSF3	0.027	1.55E-06	*ADGRE1, CX3CR1, EGR1, GATA1, GNLY, GZMB, HDC, IL4, KLRC1, KLRC2, MMP9, PROK2*	*CEACAM8, PRTN3*
IL1	2.837	1.89E-06	*ADAMTS1, ADRB2, CCL4, CHI3L1, CXCL1, CXCL9, EGR1, HP, IDO1, IL1RL1, IL4, IL5RA, LAMB2,*	*ACAN, CEACAM6, FN1, INHBA*

Table 2 (*continued*)

Upstream Regulator	Activation z-score	p-value of overlap	Target molecules (up DEGs)	Target molecules (down DEGs)
			MMP9, NRG1, NTRK1	
IL10	0.862	3.45E-06	*CCL4, CCR8, CD163, CD209, CX3CR1, CXCL9, GZMA, GZMB, IDO1, IL4, KLRD1, LZTS1, MMP14, MMP9, MS4A2, SLC1A3, TLR3, TNIP3*	*FCGR3A/FCGR3B, INHBA, MSR1, TNFRSF13B, TNFRSF13C*
SMARCA4	1.069	7.52E-06	*ALDH2, CCR8, CLIC2, CXCL1, EGR1, FFAR2, FGFR2, IL4, RETN, SERPINH1, TNFRSF10C, TNFRSF9, TREM2, TRIM36, UBD*	*CEACAM6, CXCR5, EBF1, FGF9, FN1, GPM6A, HAPLN3, INHBA, ITGA3, PHLDB1, SDC2, SPOCD1*
NEUROG1	0.707	1.09E-05	*C1orf115, CXCL1, CYSLTR2, MMP9*	*FGF9, FN1, INHBA, MTARC2*

an increase of calcium release from the ER induced by the drug.

3.9. CREB activation in SHSY-5Y cells

Immunoblotting analysis of the CREB protein was performed on SHSY-5Y cells. A significant increase in the expression of phospho-CREB was observed after treatment with thalidomide at the concentrations of 200 and 400 μM for 72 h (Fig. 10 and Fig. S8).

4. Discussion

In order to broaden the knowledge on the mechanisms of action of thalidomide, PBMCs isolated from whole blood samples of pediatric patients with IBD treated with the immunomodulator were used for transcriptome analysis. This analysis considered all IBD patients as part of the same group, regardless of the presence of CD or UC diagnosis. The rationale for this choice was based on the observation of very high inter-individual difference in response, which largely exceeded detectable differences between the two IBD subtypes. Although CD and UC patients may display, due to their different clinical condition, different responses to thalidomide, our experimental design was not adequate to appropriately address this biological question, which was however preliminarily investigated, as detailed in Data note S1. Our analysis was therefore aimed at identifying a set of core genes responsive to thalidomide treatment and shared by all IBD patients. This approach allowed the detection of a number of significant DEGs. In order to give an interpretation of their biological effect, an integrative approach, based on the analysis of the altered GO terms and IPA analysis was used. The most significant shared enriched pathways that emerged were related to the regulation of phagosome formation, chemokine activity, cytosolic calcium ion concentration, cAMP-mediated signaling, eicosanoid signaling and inhibition of matrix metalloproteinases. Many of these processes, such as regulation of phagocytosis and inhibition of extracellular matrix degradation, have been already described as pathways altered by thalidomide in vitro [33–35]. Interestingly, IPA also allowed the identification of several endogenous molecules, which can be considered as strong candidates in the regulation of DEGs. In particular, a number of pro-inflammatory cytokines and pro-angiogenic factors known to be regulated by thalidomide, such as IL2, TNF, VEGF, and TGFB1 [36,37] were identified as upstream regulators of DEGs in IBD patients. Gene expression studies were followed by CMap analyses, which permits to provide some insights about the possible mode of

Table 3
Significant perturbagens (score >50) with transcriptional profiles similar to thalidomide.

Perturbagen	Score	Connectivity Map ID	Mode of action
MLN-4924	92.07	BRD-K67844266	Nedd activating enzyme inhibitor
BNTX	81.05	BRD-A55484088	Opioid receptor antagonist
NSC-94258	79.43	BRD-K56450366	Antineoplastic
LFM-A12	78.86	BRD-A44551378	EGFR inhibitor
terreic-acid	77.25	BRD-A64228451	BTK inhibitor
QL-XII-47	76.28	BRD-U86922168	BTK inhibitor, Cytoplasmic tyrosine protein kinase BMX inhibitor
7,4′-dihydroxyflavone	70.76	BRD-K50384076	Opioid receptor antagonist
SB-269970	66.25	BRD-K24201553	Serotonin receptor antagonist
WR-216174	65.42	BRD-K26669427	PFMRK inhibitor
HNHA	64.68	BRD-K76698671	HDAC inhibitor
CAY-10585	60.88	BRD-K88551539	HIF modulator
SB-206553	59.37	BRD-K36395411	Serotonin receptor antagonist
RS-56812	58.76	BRD-K20714604	Serotonin receptor partial agonist
BI-78D3	55.82	BRD-K73982490	JNK inhibitor
radicicol	55.58	BRD-K33551950	HSP inhibitor
NF-449	54.9	BRD-K36324071	Purinergic receptor antagonist

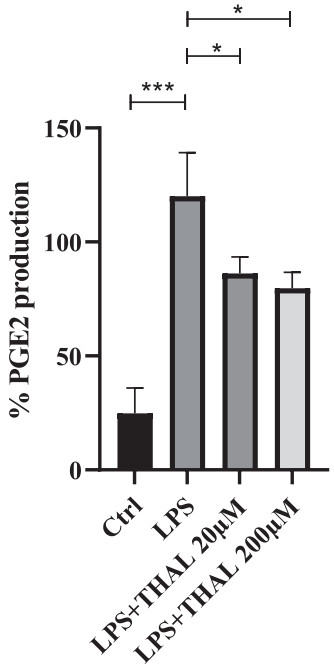

Fig. 3. PGE2 production in THP-1 macrophages. Evaluation of levels of PGE2 production in THP-1 differentiated in macrophages, unstimulated (Ctrl) or stimulated with LPS (LPS), after 72 h of treatment with 20 and 200 μM of thalidomide (THAL). The graphs represent the percentages of PGE2 production normalized on stimulated cells (LPS). One-way ANOVA: $p = 0.0001$. Tukey's multiple comparison *$p < 0.05$; * **$p < 0.001$. Data are reported as means ± SE of three independent experiments performed in quadruplicate.

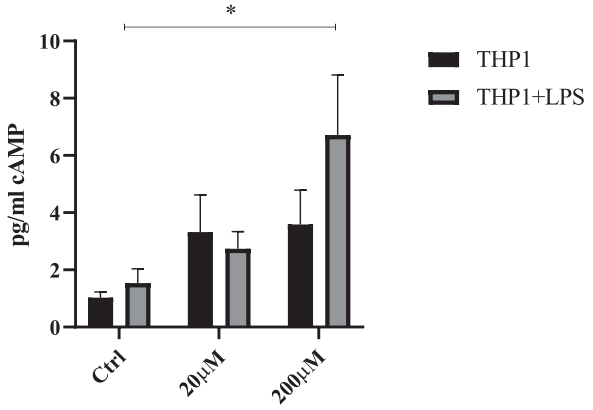

Fig. 4. Evaluation of cAMP levels in THP-1 stimulated or not with LPS after 72 h of treatment with 20 and 200 μM of thalidomide. Two-way ANOVA: column factor (Stimulation or not with LPS) p = n.s.; row factor (Thalidomide concentration) $p = 0.01$. Tukey's multiple comparison * $p < 0.05$. Data are reported as means ± SE of three independent experiments performed in quadruplicate.

action of thalidomide and reveal a few compounds that determined a gene expression profile in treated cells similar to the one we observed in this study, allowing the identification of drugs that could be potentially repurposed for the treatment of IBD patients [30]. The compound with the highest similarity score identified by this approach, MLN4924, is a small-molecule inhibitor of NEDD8 activating enzyme. By blocking the conjugation of the ubiquitin-like molecule Nedd8 to the cullin scaffold protein, MLN4924 suppresses ubiquitination activity of the E3 ligase CRL4A [38], which is responsible for protein ubiquitination and degradation [39]. Likewise, thalidomide derivatives lenalidomide and pomalidomide effects are determined by altering ubiquitination of target substrates by CRL4A-CRBN. In particular, their anti-proliferative and immunomodulatory effects in multiple myeloma cells are induced by the direct interaction with CRBN, which enhances the binding and subsequent ubiquitination of the zinc finger transcription factors, Ikaros and Aiolos [40]. The overlap of gene expression profiles induced by thalidomide in pediatric IBD patients and MLN4924 identified 128 genes commonly altered by both treatments. The functional characterization of these genes determined a main involvement in chemokine-mediated signalling pathway and immune response (Table S6). Considering the single genes commonly altered by both compounds, several (*EGR1, ANXA1, CES1, DNASE1L3, FFAR2, IDO1, IL4, MMP9, PRKCDBP, TNFRSF10C*) are regulated by Ikaros and Aiolos. The above findings suggest an interesting possibility that thalidomide and MLN4924 exert similar immunomodulatory effects as already described in IBD mouse models [41]. Moreover, these observations suggest that thalidomide could alter the substrate specificity of CRBN for proteins important in IBD among which ubiquitin-specific protease, NF-κB and TGFβ [42].

To confirm the role of candidate pathways altered by thalidomide in our cohort of patients, in vitro experiments were performed. The monocytic cell line THP-1 and THP-1-derived macrophages were employed to investigate the possible involvement of pathways emerging from RNA-seq analysis related to the immunomodulatory and anti-inflammatory effect of thalidomide. In particular, on THP-1 cells stimulated with LPS we demonstrated the ability of thalidomide to influence the eicosanoid signaling by diminishing the secretion of PGE2 in a dose-dependent manner. PGE2 is present in most tissues at biologically functional nanomolar levels, and its levels are increased in sites of

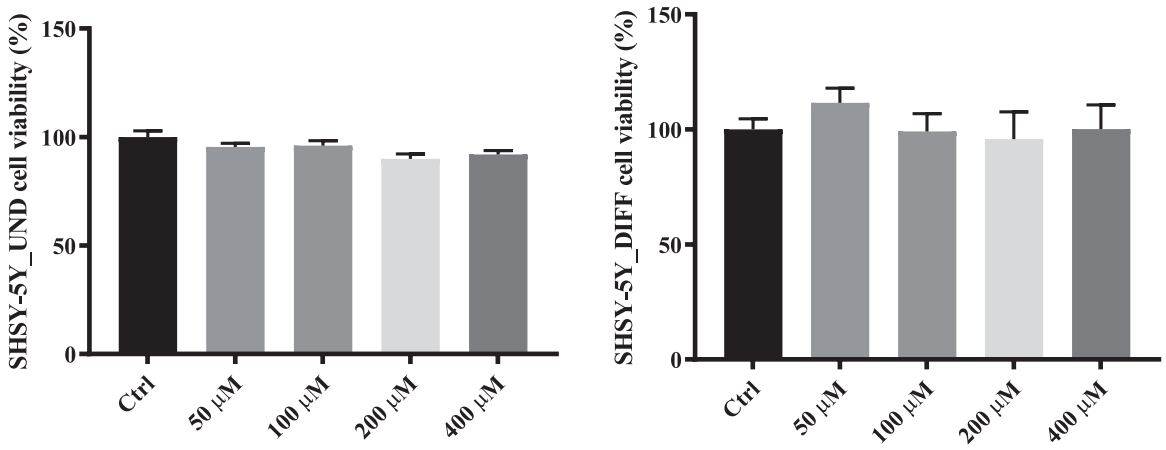

Fig. 5. Evaluation of the cytotoxic effect of thalidomide in SHSY-5Y cells. Cells differentiated (DIFF) or not (UND) were treated with thalidomide for 72 h. The percentages were calculated on the untreated cells (Ctrl). One-way ANOVA: UND p = n.s., DIFF p = n.s. Data are reported as means ± SE of three independent experiments performed in quadruplicate.

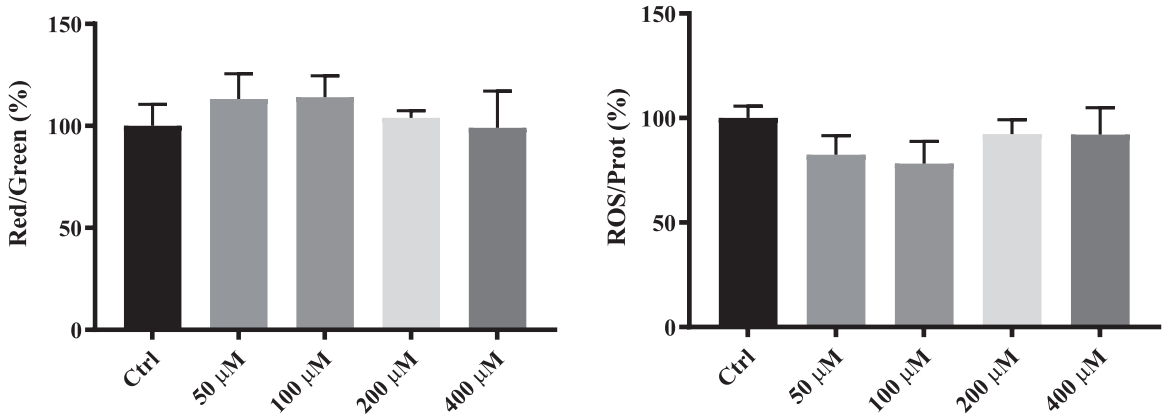

Fig. 6. Effect of thalidomide on mitochondrial membrane potential (MMP, $\Delta\Psi_m$) and ROS production in SHSY-5Y cells. Cells were treated with thalidomide for 72 h. The pictures represent the ratios of JC-1 monomeric form to JC-1 aggregates (red/green fluorescence) for untreated (Ctrl) and treated cells, normalized on untreated cells. Ratio between ROS and protein concentration was normalized on untreated cells (Ctrl). One-way ANOVA: MMP p = n.s.; ROS p = n.s. Data are reported as means ± SE of three independent experiments performed in quadruplicate.

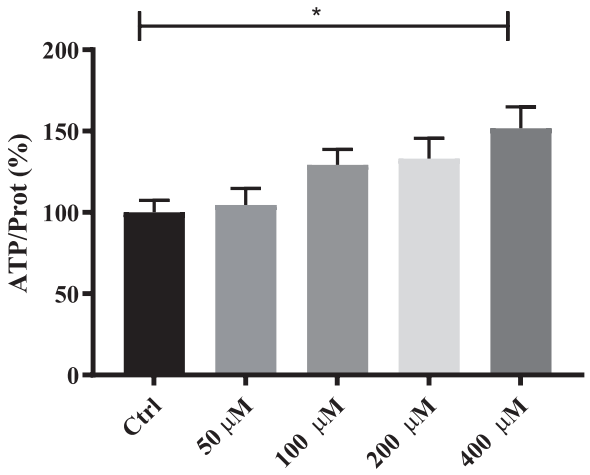

Fig. 7. ATP levels in SHSY-5Y cells treated with thalidomide. Cells were treated with thalidomide for 72 h. The percentages were calculated on the untreated cells (Ctrl). Ratio between ATP and protein concentration was normalized on untreated cells (Ctrl). One-way ANOVA: p = 0.02, Tukey's multiple comparison *p < 0.05. Data are reported as means ± SE of four independent experiments performed in quadruplicate.

inflammation [43]. Reduced levels of PGs were reported in mucosal tissue from UC patients after treatment with sulfasalazine, sulfapyridine, and 5-aminosalicylic acid [44]. Thalidomide may reduce levels of PGE2, through the modulation of enzyme prostaglandin G/H synthase activity, as described in previous works [45–47], suppressing intestinal inflammation in IBD patients.

In addition, the modulating G protein-coupled receptor (GPCR) pathway and cAMP-mediated signaling emerged from the enrichment analysis among the most significantly altered pathways. Many drugs act on GPCRs and produce their effects by increasing or decreasing the activity of adenylate cyclase, thereby modulating the production of cyclic adenosine monophosphate (cAMP) [48]. cAMP is a potent regulator of innate and adaptive immune cell functions and as a result of its increased levels a reduction of pro-inflammatory cytokines among which TNF, IL-17, and IFN-γ has been extensively described [49,50]. To demonstrate the possible alteration by thalidomide in cAMP related signaling pathways, the production of cAMP was quantified in THP-1 cells. Thalidomide led to a significant increase in cAMP levels in monocytes stimulated with LPS. This result could depend on the ability of thalidomide to inhibit phosphodiesterases (PDE), the enzymes that convert cAMP to AMP, causing an increase in cAMP. This mechanism is reminiscent of that of apremilast, sildenafil and derivatives, and analogues of thalidomide [51,52]. In particular, the efficacy of the PDE4 inhibitor apremilast in UC patients was already reported [53] indicating

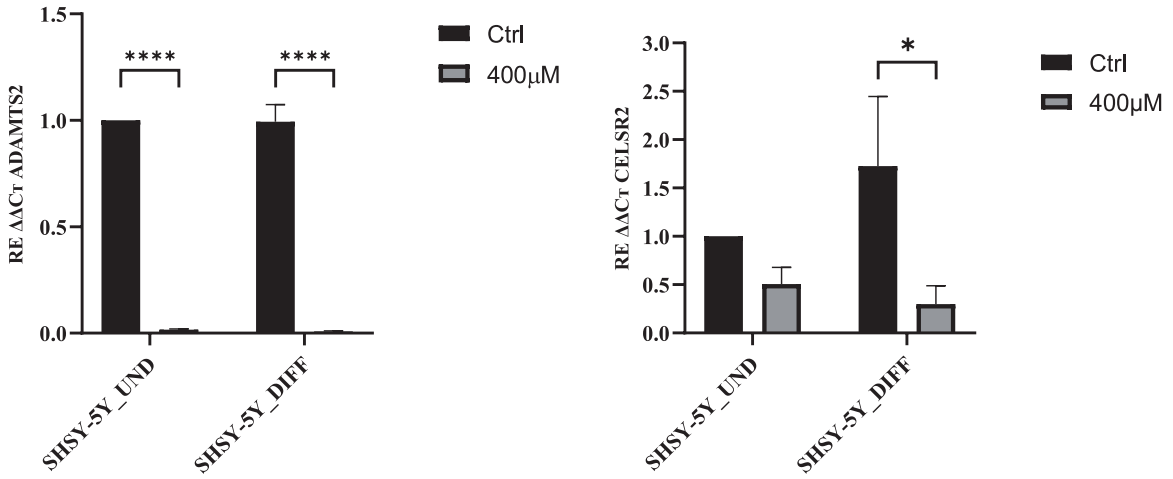

Fig. 8. Quantification of *ADAMTS2* and *CELSR2* expression levels in SHSY-5Y treated with thalidomide. *ADAMTS2* and *CELSR2* gene relative expression ($2^{-\Delta\Delta CT}$) was calculated with respect to the housekeeping *ACTB* gene on SHSY-5Y cells differentiated (DIFF) or not (UND). Two-way ANOVA: *ADAMTS2* column factor (treatment) $p < 0.0001$; *CELSR2* column factor (treatment) $p = 0.01$. Tukey's multiple comparison * $p < 0.05$; * * $p < 0.01$, * ** $p < 0.001$, * ** * $p < 0.0001$. Data are reported as means ± SE of three independent experiments performed in quadruplicate.

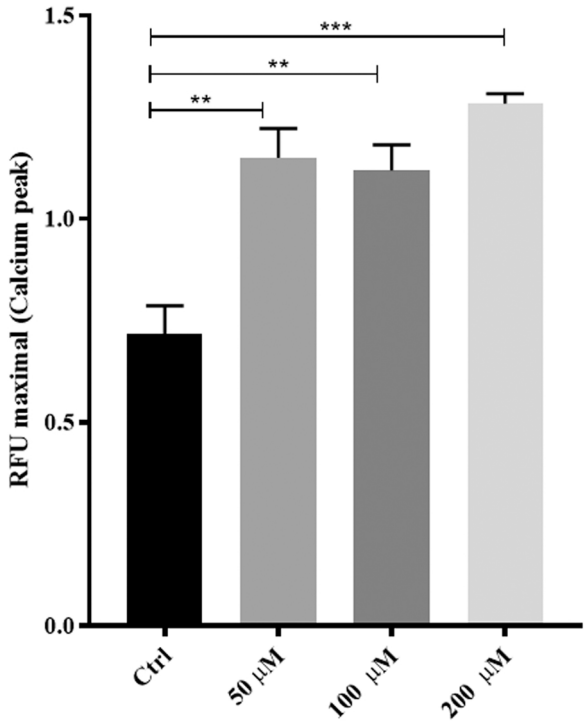

Fig. 9. Quantification of intracellular calcium. Relative expression of calcium peaks in SHSY-5Y cells treated with thalidomide (50–200 μM) for 72 h. Maximal relative fluorescence units (RFU) were normalized on baseline readings (means of first 20 s readings). Untreated cells were used as controls (Ctrl). One-way ANOVA: $p < 0.001$. Tukey's multiple comparison post-test * *$p < 0.01$, * **$p < 0.001$. Data are reported as means ± SE of three independent experiments performed in quadruplicate.

that this molecular mechanism, which leads to an increase in cAMP levels, could be important in the resolution of inflammation in IBD patients treated with thalidomide.

In addition to the pathways and genes analyzed related to the immunomodulatory mechanism of thalidomide, the hypergeometric test and IPA analysis revealed some overrepresented pathways linked to functions and components of the nervous system. Since peripheral neuropathy is one of the most frequent adverse events of thalidomide and is a common cause of treatment discontinuation [16], we considered important to verify the validity of the results obtained. For this purpose, SHSY-5Y neuronal cells, were used to evaluate the effect of thalidomide in vitro. By measuring various parameters indicative of viability such as metabolic activity and ROS production it was possible to demonstrate that thalidomide does not alter cell growth as already reported for other cell types [33,54]. Interestingly, our data seems to suggest a possible "decoupling" between ATP production and ROS production, as observed in another model of neuropathy [55]; excess intracellular ATP has been shown to be causative for neuropathic pain in spinal cord injury [56]. In the literature, the mechanisms by which drugs as chemotherapeutics lead to a peripheral neuropathy has been largely described and involves principally oxidative stress, alteration in ion channel activity, neuroinflammation, and mitochondrial damage [57] but our data suggest a different mechanism of action of thalidomide neurotoxicity. The differential expression of the top 2 downregulated genes *ADAMTS2* (ADAM Metallopeptidase With Thrombospondin Type 1 Motif 2) and *CELSR2* (Cadherin EGF LAG Seven-Pass G-Type Receptor 2) measured by RNA-seq on PBMCs of IBD patients treated with thalidomide was further demonstrated in SHSY-5Y cell line treated with the drug but no data about their role in peripheral neuropathy have been published. ADAMTS2 is a secreted metalloproteinase which excises the N-propeptide of the fibrillar procollagens types I-III and type V [58] and its transcription is primarily controlled by the cAMP/CREB signalling [59]. This pathway resulted deregulated by thalidomide as reported from IPA analysis. Moreover, increasing evidence suggests the role of ADAMTS family proteins in neuroplasticity [60]. CELSR2, an atypical cadherine, is involved in neuron axon growth and regeneration [61,62] and its upregulation has been observed after peripheral nerve injury [62]. Regarding the mechanisms of these two proteins in thalidomide-induced peripheral neuropathy, further investigation is needed.

Considering the number of biological processes related to the calcium signaling and transport obtained from GO and IPA analysis, intracellular calcium (Ca^{2+}) was measured in SHSY-5Y cells treated with thalidomide for 72 h. The results demonstrated a significant increase of intracellular calcium after stimulation with thapsigargin, an inhibitor of sarco(endo) plasmic reticulum Ca^{2+} ATP-ase (SERCA), underlying an effect of thalidomide on calcium homeostasis. In the literature, the effect of thalidomide on intracellular calcium levels is currently poorly studied, in particular in neuronal cell models. Abnormal neuronal calcium homeostasis has been implicated in numerous diseases of the nervous system, including peripheral neuropathies induced by chemotherapy [63]. Increased cytosolic calcium concentrations initiate the activation

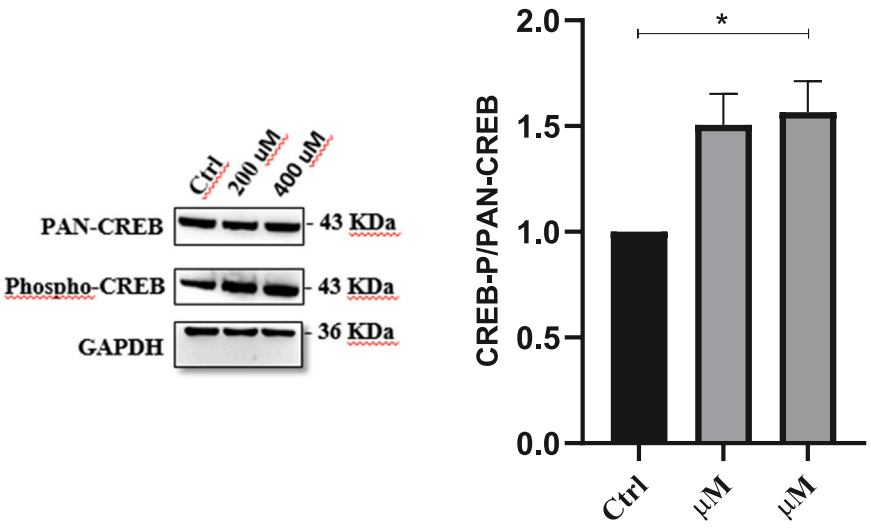

Fig. 10. PAN-CREB and phospho-CREB (P-CREB) protein expression in SHSY-5Y cells treated with thalidomide. Protein lysates were obtained from SHSY-5Y cells treated with thalidomide 0 (Ctrl), 200 and 400 µM for 72 h. GAPDH was used as internal control. Representative western blot image of one of three replicates. Statistical analysis: One-way ANOVA: $p = 0.03$; Tukey's multiple comparison: $^*p < 0.05$.

of several kinase-dependent signalling cascades leading to CREB activation [64], an overrepresented pathway emerged with IPA. Indeed, our study demonstrated that thalidomide increased CREB activation in SHSY-5Y cells, confirming the crucial role of these pathways in thalidomide action. Further experiments will be needed to investigate the downstream effects of this Ca^{2+} increment after thalidomide treatment in neuronal cells. In the future, an in-depth analysis of the altered pathways emerged from our work should also be validated on different cellular models such as IBD patient-derived intestinal organoids to obtain more information regarding the mechanism of action of thalidomide at the epithelial tissue level.

This study has some limitations regarding the relatively small size of the cohort that for instance prevents adjusting the analysis for the different disease type (CD and UC). Future investigations should be addressed in a larger number of pediatric patients affected by IBD, to highlight differentially expressed genes and altered pathways by thalidomide in CD and UC.

An additional limitation is related to the tissue (PBMCs) used to conduct the transcriptomic analysis. Even though a mixed cells analysis is suboptimal, since differences in gene expression can be driven by differences in the cellular composition of starting material, the investigation of gene expression in PBMCs represents a simple approach with diagnostic purpose, and easier to translate in clinical practice. In the future, it will be important to evaluate the effect of thalidomide also in other cell types such as intestinal epithelium, due to the important role of this tissue in IBD pathogenesis [1]. Moreover, in order to improve our knowledge on the mechanism of thalidomide-induced neuropathy, neuronally-derived extracellular vesicles could be an innovative tool for better understanding the molecular basis of this adverse event [65].

In conclusion, exploring thalidomide-induced alterations in gene expression in pediatric patients with IBD allowed to elucidate its mechanism of action, highlighting that the ubiquitin-proteasome pathway is an important target for the immunomodulatory effects. The transcriptomic analysis provides the molecular basis for the identification of biomarkers associated with efficacy and/or adverse events related to thalidomide treatment in pediatric IBD patients useful for therapy personalization. Most of the overrepresented pathway emerged with in silico analysis can be recapitulated in vitro providing a valuable tool to fill up a significant gap in understanding the molecular mechanism of thalidomide. Understanding the underlying mechanisms of thalidomide-induced peripheral neuropathy could be useful to prevent the onset of this complication and to treat the most severe symptoms. Personalization of therapy based on this information will result in higher quality of life, lower toxicity, and a more rational treatment.

Institutional review board statement

The study was conducted in accordance with the Declaration of Helsinki, and approved by the Regional Ethics Committee (CEUR) of Friuli Venezia Giulia with identification code CEUR-2017-Sper-031 and CEUR-2019-Sper-105.

Funding

This work was supported by the Italian Ministry of Health, through the contribution given to the Institute for Maternal and Child Health IRCCS Burlo Garofolo, Trieste, Italy, grant NET-2013–02355002 and RC 15/23.

CRediT authorship contribution statement

Marianna Lucafò, Matteo Bramuzzo and Gabriele Stocco: study conception and design. **Letizia Pugnetti, Debora Curci, Carlotta Bidoli, Marco Gerdol, Fulvio Celsi, Sara Renzi, Monica Paci, Sara Lega, Martina Nonnis, Paolo Lionetti, Alessandra Maestro, Liza Vecchi Brumatti, Paolo Edomi, Danilo Licastro and Matteo Bramuzzo:** acquisition, analysis, and interpretation of the data. **Marianna Lucafò, Letizia Pugnetti, Debora Curci and Carlotta Bidoli:** drafted the initial manuscript. **Gabriele Stocco, Giuliana Decorti, Marianna Lucafò and Matteo Bramuzzo:** critical discussion. **Gabriele Stocco, Marianna Lucafò and Matteo Bramuzzo:** study supervision. All authors contributed to the article and approved the submitted version.

Declaration of Competing Interest

The authors declare that they have no known competing financial interests or personal relationships that could have appeared to influence the work reported in this paper.

Data Availability

Data and study materials will be made available to other researchers upon motivated request to the corresponding author.

Appendix A. Supporting information

Supplementary data associated with this article can be found in the online version at doi:10.1016/j.biopha.2023.114927.

References

[1] J.T. Chang, Pathophysiology of inflammatory bowel diseases, N. Engl. J. Med 383 (2020) 2652–2664, https://doi.org/10.1056/NEJMra2002697.

[2] L. Rigoli, R.A. Caruso, Inflammatory bowel disease in pediatric and adolescent patients: a biomolecular and histopathological review, World J. Gastroenterol. 20 (2014) 10262–10278, https://doi.org/10.3748/wjg.v20.i30.10262.

[3] M.J. Rosen, A. Dhawan, S.A. Saeed, Inflammatory bowel disease in children and adolescents, JAMA Pedia 169 (2015) 1053–1060, https://doi.org/10.1001/jamapediatrics.2015.1982.

[4] S.B. Oliveira, I.M. Monteiro, Diagnosis and management of inflammatory bowel disease in children, Bmj 357 (2017) j2083, https://doi.org/10.1136/bmj.j2083.

[5] Z. Cai, S. Wang, J. Li, Treatment of inflammatory bowel disease: a comprehensive review, Front Med (Lausanne) 8 (2021), 765474, https://doi.org/10.3389/fmed.2021.765474.

[6] L.B. Grossberg, K. Papamichael, A.S. Cheifetz, Review article: emerging drug therapies in inflammatory bowel disease, Aliment Pharm. Ther. 55 (2022) 789–804, https://doi.org/10.1111/apt.16785.

[7] M. Lucafò, M. Bramuzzo, D. Selvestrel, P. Da Lozzo, G. Decorti, G. Stocco, Gender may influence the immunosuppressive actions of prednisone in young patients with inflammatory bowel disease, Front Immunol. 12 (2021), 673068, https://doi.org/10.3389/fimmu.2021.673068.

[8] M. Lucafò, R. Franca, D. Selvestrel, D. Curci, L. Pugnetti, G. Decorti, G. Stocco, Pharmacogenetics of treatments for inflammatory bowel disease, Expert Opin. Drug Metab. Toxicol. 14 (2018) 1209–1223, https://doi.org/10.1080/17425255.2018.1551876.

[9] G. Stelzer, N. Rosen, I. Plaschkes, S. Zimmerman, M. Twik, S. Fishilevich, T.I. Stein, R. Nudel, I. Lieder, Y. Mazor, et al., The GeneCards suite: from gene data mining to disease genome sequence analyses, 1.30.31-31.30.33, Curr. Protoc. Bioinforma. 54 (2016), https://doi.org/10.1002/cpbi.5.

[10] C.S. Yang, C. Kim, R.J. Antaya, Review of thalidomide use in the pediatric population, J. Am. Acad. Dermatol. 72 (2015) 703–711, https://doi.org/10.1016/j.jaad.2015.01.002.

[11] G.G. Amare, B.G. Meharie, Y.M. Belayneh, A drug repositioning success: the repositioned therapeutic applications and mechanisms of action of thalidomide, J. Oncol. Pharm. Pr. 27 (2021) 673–678, https://doi.org/10.1177/1078155220975825.

[12] M. Bramuzzo, A. Ventura, S. Martelossi, M. Lazzerini, Thalidomide for inflammatory bowel disease: Systematic review, Med. (Baltim.) 95 (2016), e4239, https://doi.org/10.1097/md.0000000000004239.

[13] M. Lazzerini, S. Martelossi, G. Magazzù, S. Pellegrino, M.C. Lucanto, A. Barabino, A. Calvi, S. Arrigo, P. Lionetti, M. Lorusso, et al., Effect of thalidomide on clinical remission in children and adolescents with refractory Crohn disease: a randomized clinical trial, Jama 310 (2013) 2164–2173, https://doi.org/10.1001/jama.2013.280777.

[14] M. Lazzerini, S. Martelossi, G. Magazzù, S. Pellegrino, M.C. Lucanto, A. Barabino, A. Calvi, S. Arrigo, P. Lionetti, M. Lorusso, et al., Effect of thalidomide on clinical remission in children and adolescents with ulcerative colitis refractory to other immunosuppressives: pilot randomized clinical trial, Inflamm. Bowel Dis. 21 (2015) 1739–1749, https://doi.org/10.1097/mib.0000000000000437.

[15] M. Lazzerini, V. Villanacci, M.C. Pellegrin, S. Martelossi, G. Magazzù, S. Pellegrino, M.C. Lucanto, A. Barabino, A. Calvi, S. Arrigo, et al., Endoscopic and histologic healing in children with inflammatory bowel diseases treated with thalidomide, e1381, Clin. Gastroenterol. Hepatol. 15 (2017) 1382–1389, https://doi.org/10.1016/j.cgh.2017.02.029.

[16] M. Bramuzzo, G. Stocco, M. Montico, S. Arrigo, A. Calvi, P. Lanteri, S. Costa, S. Pellegrino, G. Magazzù, J. Barp, et al., Risk factors and outcomes of thalidomide-induced peripheral neuropathy in a pediatric inflammatory bowel disease cohort, Inflamm. Bowel Dis. 23 (2017) 1810–1816, https://doi.org/10.1097/mib.0000000000001195.

[17] P. Tacchetti, C. Terragna, M. Galli, E. Zamagni, M.T. Petrucci, A. Pezzi, V. Montefusco, M. Martello, P. Tosi, L. Baldini, et al., Bortezomib- and thalidomide-induced peripheral neuropathy in multiple myeloma: clinical and molecular analyses of a phase 3 study, Am. J. Hematol. 89 (2014) 1085–1091, https://doi.org/10.1002/ajh.23835.

[18] T. Ito, H. Ando, T. Suzuki, T. Ogura, K. Hotta, Y. Imamura, Y. Yamaguchi, H. Handa, Identification of a primary target of thalidomide teratogenicity, Science 327 (2010) 1345–1350, https://doi.org/10.1126/science.1177319.

[19] S. Angers, T. Li, X. Yi, M.J. MacCoss, R.T. Moon, N. Zheng, Molecular architecture and assembly of the DDB1-CUL4A ubiquitin ligase machinery, Nature 443 (2006) 590–593, https://doi.org/10.1038/nature05175.

[20] K.A. Donovan, J. An, R.P. Nowak, J.C. Yuan, E.C. Fink, B.C. Berry, B.L. Ebert, E. S. Fischer, Thalidomide promotes degradation of SALL4, a transcription factor implicated in duane radial ray syndrome, Elife (2018) *7*, https://doi.org/10.7554/eLife.38430.

[21] C. Fionda, M.P. Abruzzese, A. Zingoni, F. Cecere, E. Vulpis, G. Peruzzi, A. Soriani, R. Molfetta, R. Paolini, M.R. Ricciardi, et al., The IMiDs targets IKZF-1/3 and IRF4 as novel negative regulators of NK cell-activating ligands expression in multiple myeloma, Oncotarget 6 (2015) 23609–23630, https://doi.org/10.18632/oncotarget.4603.

[22] M.E. Matyskiela, W. Zhang, H.W. Man, G. Muller, G. Khambatta, F. Baculi, M. Hickman, L. LeBrun, B. Pagarigan, G. Carmel, et al., A cereblon modulator (CC-220) with improved degradation of ikaros and aiolos, J. Med Chem. 61 (2018) 535–542, https://doi.org/10.1021/acs.jmedchem.6b01921.

[23] Q.L. Sievers, G. Petzold, R.D. Bunker, A. Renneville, M. Słabicki, B.J. Liddicoat, W. Abdulrahman, T. Mikkelsen, B.L. Ebert, N.H. Thomä, Defining the human C2H2 zinc finger degrome targeted by thalidomide analogs through CRBN, Science (2018) *362*, https://doi.org/10.1126/science.aat0572.

[24] Y.X. Zhu, E. Braggio, C.X. Shi, K.M. Kortuem, L.A. Bruins, J.E. Schmidt, X.B. Chang, P. Langlais, M. Luo, P. Jedlowski, et al., Identification of cereblon-binding proteins and relationship with response and survival after IMiDs in multiple myeloma, Blood 124 (2014) 536–545, https://doi.org/10.1182/blood-2014-02-557819.

[25] A.L. Moreira, E.P. Sampaio, A. Zmuidzinas, P. Frindt, K.A. Smith, G. Kaplan, Thalidomide exerts its inhibitory action on tumor necrosis factor alpha by enhancing mRNA degradation, J. Exp. Med 177 (1993) 1675–1680, https://doi.org/10.1084/jem.177.6.1675.

[26] S. Majumdar, B. Lamothe, B.B. Aggarwal, Thalidomide suppresses NF-kappa B activation induced by TNF and H2O2, but not that activated by ceramide, lipopolysaccharides, or phorbol ester, J. Immunol. 168 (2002) 2644–2651, https://doi.org/10.4049/jimmunol.168.6.2644.

[27] G.P. Wagner, K. Kin, V.J. Lynch, Measurement of mRNA abundance using RNA-seq data: RPKM measure is inconsistent among samples, Theory Biosci. 131 (2012) 281–285, https://doi.org/10.1007/s12064-012-0162-3.

[28] S. Falcon, R. Gentleman, Using GOstats to test gene lists for GO term association, Bioinformatics 23 (2007) 257–258, https://doi.org/10.1093/bioinformatics/btl567.

[29] A. Krämer, J. Green, J. Pollard Jr, S. Tugendreich, Causal analysis approaches in Ingenuity Pathway Analysis, Bioinformatics 30 (2014) 523–530, https://doi.org/10.1093/bioinformatics/btt703.

[30] A. Subramanian, R. Narayan, S.M. Corsello, D.D. Peck, T.E. Natoli, X. Lu, J. Gould, J.F. Davis, A.A. Tubelli, J.K. Asiedu, et al., A next generation connectivity map: L1000 platform and the first 1,000,000 profiles, e1417, Cell 171 (2017) 1437–1452, https://doi.org/10.1016/j.cell.2017.10.049.

[31] M. Lucafò, L. Pugnetti, M. Bramuzzo, D. Curci, A. Di Silvestre, A. Marcuzzi, A. Bergamo, S. Martelossi, V. Villanacci, A. Bozzola, et al., Long non-coding RNA GAS5 and intestinal MMP2 and MMP9 expression: a translational study in pediatric patients with IBD, Int J. Mol. Sci. (2019) *20*, https://doi.org/10.3390/ijms20215280.

[32] T. Kume, Y. Kawato, F. Osakada, Y. Izumi, H. Katsuki, T. Nakagawa, S. Kaneko, T. Niidome, Y. Takada-Takatori, A. Akaike, Dibutyryl cyclic AMP induces differentiation of human neuroblastoma SH-SY5Y cells into a noradrenergic phenotype, Neurosci. Lett. 443 (2008) 199–203, https://doi.org/10.1016/j.neulet.2008.07.079.

[33] R.L. Barnhill, N.J. Doll, L.E. Millikan, R.C. Hastings, Studies on the anti-inflammatory properties of thalidomide: effects on polymorphonuclear leukocytes and monocytes, J. Am. Acad. Dermatol. 11 (1984) 814–819, https://doi.org/10.1016/s0190-9622(84)80458-2.

[34] S. Gao, S. Wang, R. Fan, J. Hu, Recent advances in the molecular mechanism of thalidomide teratogenicity, Biomed. Pharm. 127 (2020), 110114, https://doi.org/10.1016/j.biopha.2020.110114.

[35] M. Gelati, E. Corsini, S. Frigerio, B. Pollo, G. Broggi, D. Croci, A. Silvani, A. Boiardi, A. Salmaggi, Effects of thalidomide on parameters involved in angiogenesis: an in vitro study, J. Neurooncol 64 (2003) 193–201, https://doi.org/10.1023/a:1025618022921.

[36] T. Liu, F. Guo, X. Zhu, X. He, L. Xie, Thalidomide and its analogues: a review of the potential for immunomodulation of fibrosis diseases and opthalmopathy, Exp. Ther. Med 14 (2017) 5251–5257, https://doi.org/10.3892/etm.2017.5209.

[37] X.L. Zhou, P. Xu, H.H. Chen, Y. Zhao, J. Shen, C. Jiang, S. Jiang, S.Z. Ni, B. Xu, L. Li, Thalidomide inhibits TGF-β1-induced epithelial to mesenchymal transition in alveolar epithelial cells via smad-dependent and smad-independent signaling pathways, Sci. Rep. 7 (2017) 14727, https://doi.org/10.1038/s41598-017-15239-2.

[38] T.A. Soucy, P.G. Smith, M.A. Milhollen, A.J. Berger, J.M. Gavin, S. Adhikari, J. E. Brownell, K.E. Burke, D.P. Cardin, S. Critchley, et al., An inhibitor of NEDD8-activating enzyme as a new approach to treat cancer, Nature 458 (2009) 732–736, https://doi.org/10.1038/nature07884.

[39] M.D. Petroski, R.J. Deshaies, Function and regulation of cullin-RING ubiquitin ligases, Nat. Rev. Mol. Cell Biol. 6 (2005) 9–20, https://doi.org/10.1038/nrm1547.

[40] G. Lu, R.E. Middleton, H. Sun, M. Naniong, C.J. Ott, C.S. Mitsiades, K.K. Wong, J. E. Bradner, W.G. Kaelin Jr., The myeloma drug lenalidomide promotes the cereblon-dependent destruction of Ikaros proteins, Science 343 (2014) 305–309, https://doi.org/10.1126/science.1244917.

[41] M. Cheng, S. Hu, Z. Wang, Y. Pei, R. Fan, X. Liu, L. Wang, J. Zhou, S. Zheng, T. Zhang, et al., Inhibition of neddylation regulates dendritic cell functions via Deptor accumulation driven mTOR inactivation, Oncotarget 7 (2016) 35643–35654, https://doi.org/10.18632/oncotarget.9543.

[42] R. Chen, X. Pang, L. Li, Z. Zeng, M. Chen, S. Zhang, Ubiquitin-specific proteases in inflammatory bowel disease-related signalling pathway regulation, Cell Death Dis. 13 (2022) 139, https://doi.org/10.1038/s41419-022-04566-6.

[43] C. Yao, S. Narumiya, Prostaglandin-cytokine crosstalk in chronic inflammation, Br. J. Pharm. 176 (2019) 337–354, https://doi.org/10.1111/bph.14530.

[44] P. Sharon, M. Ligumsky, D. Rachmilewitz, U. Zor, Role of prostaglandins in ulcerative colitis. Enhanced production during active disease and inhibition by sulfasalazine, *Gastroenterology* 75 (1978) 638–640.
[45] R.R. Arlen, P.G. Wells, Inhibition of thalidomide teratogenicity by acetylsalicylic acid: evidence for prostaglandin H synthase-catalyzed bioactivation of thalidomide to a teratogenic reactive intermediate, J. Pharm. Exp. Ther. 277 (1996) 1649–1658.
[46] C.J. Lee, L.L. Gonçalves, P.G. Wells, Embryopathic effects of thalidomide and its hydrolysis products in rabbit embryo culture: evidence for a prostaglandin H synthase (PHS)-dependent, reactive oxygen species (ROS)-mediated mechanism, Faseb J. 25 (2011) 2468–2483, https://doi.org/10.1096/fj.10-178814.
[47] F. Payvandi, L. Wu, M. Haley, P.H. Schafer, L.H. Zhang, R.S. Chen, G.W. Muller, D. I. Stirling, Immunomodulatory drugs inhibit expression of cyclooxygenase-2 from TNF-alpha, IL-1beta, and LPS-stimulated human PBMC in a partially IL-10-dependent manner, Cell Immunol. 230 (2004) 81–88, https://doi.org/10.1016/j.cellimm.2004.09.003.
[48] A.S. Hauser, C. Avet, C. Normand, A. Mancini, A. Inoue, M. Bouvier, D.E. Gloriam, Common coupling map advances GPCR-G protein selectivity, Elife (2022) *11*, https://doi.org/10.7554/eLife.74107.
[49] A. Picchianti-Diamanti, F.R. Spinelli, M.M. Rosado, F. Conti, B. Laganà, Inhibition of Phosphodiesterase-4 in Psoriatic Arthritis and Inflammatory Bowel Diseases, Int J. Mol. Sci. (2021) *22*, https://doi.org/10.3390/ijms22052638.
[50] V.K. Raker, C. Becker, K. Steinbrink, The cAMP pathway as therapeutic target in autoimmune and inflammatory diseases, Front Immunol. 7 (2016) 123, https://doi.org/10.3389/fimmu.2016.00123.
[51] G.W. Muller, M.G. Shire, L.M. Wong, L.G. Corral, R.T. Patterson, Y. Chen, D. I. Stirling, Thalidomide analogs and PDE4 inhibition, Bioorg. Med Chem. Lett. 8 (1998) 2669–2674, https://doi.org/10.1016/s0960-894x(98)00475-2.
[52] V.M. Muñoz-Pérez, E. Fernández-Martínez, H. Ponce-Monter, M.I. Ortiz, Relaxant and anti-inflammatory effect of two thalidomide analogs as PDE-4 inhibitors in pregnant rat uterus, Korean J. Physiol. Pharm. 21 (2017) 429–437, https://doi.org/10.4196/kjpp.2017.21.4.429.
[53] S. Danese, M.F. Neurath, A. Kopoń, S.F. Zakko, T.C. Simmons, R. Fogel, C.A. Siegel, R. Panaccione, X. Zhan, K. Usiskin, et al., Effects of apremilast, an oral inhibitor of phosphodiesterase 4, in a randomized trial of patients with active ulcerative colitis, e2529, Clin. Gastroenterol. Hepatol. 18 (2020) 2526–2534, https://doi.org/10.1016/j.cgh.2019.12.032.
[54] E. Genova, F. Cavion, M. Lucafò, M. Pelin, G. Lanzi, S. Masneri, R.M. Ferraro, E. M. Fazzi, S. Orcesi, G. Decorti, et al., Biomarkers and precision therapy for primary immunodeficiencies: an In Vitro study based on induced pluripotent stem cells from patients, Clin. Pharm. Ther. 108 (2020) 358–367, https://doi.org/10.1002/cpt.1837.
[55] G. van Hameren, G. Campbell, M. Deck, J. Berthelot, B. Gautier, P. Quintana, R. Chrast, N. Tricaud, In vivo real-time dynamics of ATP and ROS production in axonal mitochondria show decoupling in mouse models of peripheral neuropathies, Acta Neuropathol. Commun. 7 (2019) 86, https://doi.org/10.1186/s40478-019-0740-4.
[56] N. Nakajima, Y. Ohnishi, M. Yamamoto, D. Setoyama, H. Imai, T. Takenaka, M. Matsumoto, K. Hosomi, Y. Saitoh, H. Furue, et al., Excess intracellular ATP causes neuropathic pain following spinal cord injury, Cell Mol. Life Sci. 79 (2022) 483, https://doi.org/10.1007/s00018-022-04510-z.
[57] A. Areti, V.G. Yerra, V. Naidu, A. Kumar, Oxidative stress and nerve damage: role in chemotherapy induced peripheral neuropathy, Redox Biol. 2 (2014) 289–295, https://doi.org/10.1016/j.redox.2014.01.006.
[58] M. Bekhouche, A. Colige, The procollagen N-proteinases ADAMTS2, 3 and 14 in pathophysiology, Matrix Biol. 44–46 (2015) 46–53, https://doi.org/10.1016/j.matbio.2015.04.001.
[59] F. Ruso-Julve, A. Pombero, F. Pilar-Cuéllar, N. García-Díaz, R. Garcia-Lopez, M. Juncal-Ruiz, E. Castro, Á. Díaz, J. Vazquez-Bourgón, A. García-Blanco, et al., Dopaminergic control of ADAMTS2 expression through cAMP/CREB and ERK: molecular effects of antipsychotics, Transl. Psychiatry 9 (2019) 306, https://doi.org/10.1038/s41398-019-0647-7.
[60] P.E. Gottschall, M.D. Howell, ADAMTS expression and function in central nervous system injury and disorders, Matrix Biol. 44–46 (2015) 70–76, https://doi.org/10.1016/j.matbio.2015.01.014.
[61] Q. Wen, H. Weng, T. Liu, L. Yu, T. Zhao, J. Qin, S. Li, Q. Wu, F. Tissir, Y. Qu, et al., Inactivating Celsr2 promotes motor axon fasciculation and regeneration in mouse and human, Brain 145 (2022) 670–683, https://doi.org/10.1093/brain/awab317.
[62] X. Zhou, Z. Zhan, C. Tang, J. Li, X. Zheng, S. Zhu, J. Qi, Silencing Celsr2 inhibits the proliferation and migration of Schwann cells through suppressing the Wnt/β-catenin signaling pathway, Biochem Biophys. Res Commun. 533 (2020) 623–630, https://doi.org/10.1016/j.bbrc.2020.09.015.
[63] C. Siau, G.J. Bennett, Dysregulation of cellular calcium homeostasis in chemotherapy-evoked painful peripheral neuropathy, Anesth. Analg. 102 (2006) 1485–1490, https://doi.org/10.1213/01.ane.0000204318.35194.ed.
[64] P. Marambaud, U. Dreses-Werringloer, V. Vingtdeux, Calcium signaling in neurodegeneration, Mol. Neurodegener. 4 (2009) 20, https://doi.org/10.1186/1750-1326-4-20.
[65] M. Shi, L. Sheng, T. Stewart, C.P. Zabetian, J. Zhang, New windows into the brain: Central nervous system-derived extracellular vesicles in blood, Prog. Neurobiol. 175 (2019) 96–106, https://doi.org/10.1016/j.pneurobio.2019.01.005.